Title

Mechanistic Insights into the Formation of the 6,10-Bicyclic Eunicellane Skeleton by the Bacterial Diterpene Synthase Bnd4

Journal

Angewandte Chemie International Edition, 60(43)

ISSN

1433-7851

Authors

Xu, Baofu
Tantillo, Dean J
Rudolf, Jeffrey D

Publication Date

2021-10-18

DOI

10.1002/anie.202109641

Peer reviewed

HHS Public Access

Author manuscript

Angew Chem Int Ed Engl. Author manuscript; available in PMC 2022 October 18.

Published in final edited form as:

Angew Chem Int Ed Engl. 2021 October 18; 60(43): 23159–23163. doi:10.1002/anie.202109641.

Mechanistic Insights into the Formation of the 6,10-Bicyclic Eunicellane Skeleton by the Bacterial Diterpene Synthase Bnd4

Baofu Xu[a], **Dean J. Tantillo**[b], **Jeffrey D. Rudolf**[a]

[a]Department of Chemistry, University of Florida, Gainesville, Florida 32611 (USA)

[b]Department of Chemistry, University of California–Davis, Davis, California 95616

Abstract

The eunicellane diterpenoids are a unique family of natural products seen in marine organisms, plants, and bacteria. We used a series of biochemical, bioinformatics, and theoretical experiments to investigate the mechanism of the first diterpene synthase known to form the eunicellane skeleton. Deuterium labeling studies and quantum chemical calculations support that Bnd4, from *Streptomyces* sp. (CL12–4), forms the 6,10-bicyclic skeleton through a 1,10-cyclization, 1,3-hydride shift, and 1,14-cyclization cascade. Bnd4 also demonstrated sesquiterpene cyclase activity and the ability to prenylate small molecules. Bnd4 possesses a unique D^{94}NxxxD motif and mutation experiments confirmed an absolute requirement for D94 as well as E169.

Graphical Abstrat

jrudolf@chem.ufl.edu .

Supporting information for this article is given via a link at the end of the document

Conflict of interest

The authors declare no conflict of interest.

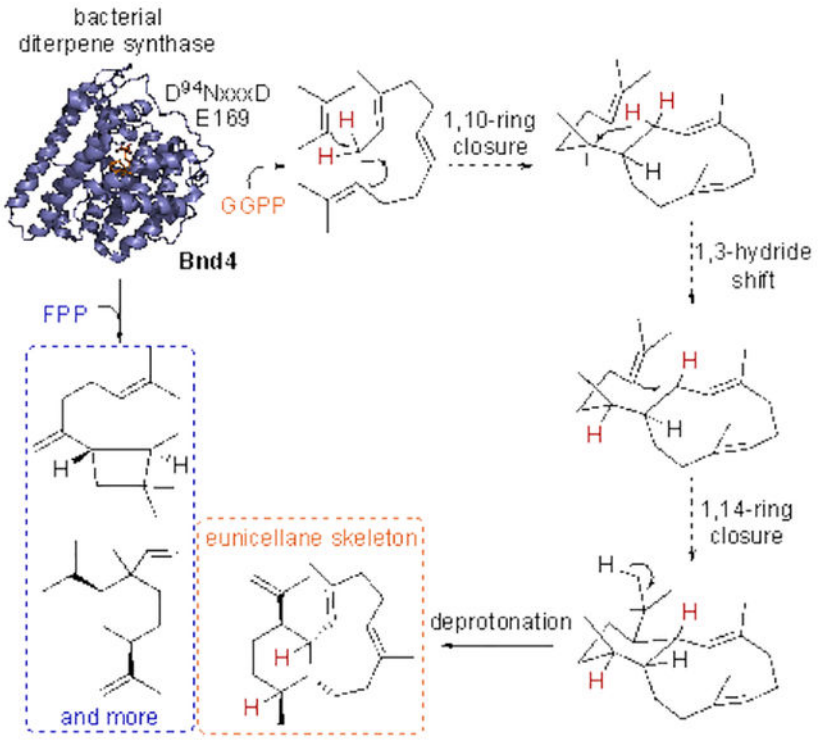

Enzymatic and mechanistic characterization of Bnd4, a bacterial diterpene synthase and the first terpene synthase known to form the 6,10-bicyclic eunicellane skeleton. Isotope labeling experiments and quantum chemical calculations support the cyclization mechanism for benditerpe-2,6,15-triene. An unusual DNxxxD motif was found to be essential for cyclization activity.

Keywords

bacterial terpenoids; enzymes; mechanism; quantum chemical calculations; terpene synthase

The eunicellane diterpenoids, a subfamily of cembranoids, possess a structurally unique 6,10-bicyclic skeleton with diverse oxidation patterns. Of the 360 reported eunicellane diterpenoids,[1] the vast majority have been found in marine Octocorallia[2–4] with only a handful isolated from plants[5,6] and, very recently, bacteria (Figure 1).[7,8] This family of natural products displays a wide range of biological activities including anti-inflammatory, anticancer, antibacterial, and antifouling properties,[2,3,7,8] making them intriguing candidates for pharmaceutical and agricultural applications as well as important but challenging targets for total synthesis.[2–4,9,10] Biosynthetic studies of the eunicellanes are non-existent, however, due to the lack of available (meta)genomes of corals and other marine organisms. In collaboration with Prof. Loesgen and colleagues, our recent discovery of benditerpenoic acid from *Streptomyces* sp. (CL12–4), its biosynthetic gene cluster, and the terpene synthase (TS) responsible for constructing its hydrocarbon core,[7] provided an excellent opportunity to investigate the enzymatic mechanism of the formation of the eunicellane skeleton. Here, we report mechanistic insights of Bnd4, the first di-TS

known to produce the eunicellane skeleton, using a series of biochemical and bioinformatic experiments and quantum chemical calculations.

Bnd4 converts geranylgeranyl diphosphate (GGPP; C20) into benditerpe-2,6,15-triene (**1**) in the biosynthesis of benditerpenoic acid (Scheme 1).[7] We also previously showed that Bnd4, along with other bacterial di-TSs, is able to prenylate small molecule nucleophiles using dimethylallyl diphosphate (DMAPP; C5) or geranyl diphosphate (GPP; C10) as prenyl donors (Figure S1).[11] Here, we additionally examined if Bnd4 was able to cyclize farnesyl diphosphate (FPP; C15) or geranylfarnesyl diphosphate (GFPP; C25). Incubation of recombinant Bnd4 with FPP yielded a series of sesquiterpenes (Figure S1C). Analysis of the C15 products using GC-MS and comparison with the NIST database annotated the six major products as β-elemene, caryo-phyllene, β-farnesene, elemol, trans-nerolidol, and epi-cubebol (Figure S2). With some exceptions,[12–15] bacterial di-TSs are not well known to possess significant sesqui-TS cyclization activity. Thus, we tested CotB2, a model bacterial di-TS that was reported to not cyclize FPP.[16] CotB2, in the presence of 1 mM FPP, produced an array of sesquiterpenes with major products including farnesol, α-farnesene, and five of the six products seen with Bnd4 (Figure S2). Finally, using an *Escherichia coli* GFPP production system, we found that Bnd4 also had sester-TS activity, although the yield was too low to isolate the product (Figure S3).

We next sought to investigate the mechanism by which the 6,10-bicyclic eunicellane skeleton is formed. Based on the overall skeleton, we initially proposed two possible cyclization cascades (Figure 2A). Pathway (i) first forms the 10-membered ring with an initial 1,10-ring closure followed by a 1,3-hydride shift (C-1 to C-11), 1,14-ring closure, and deprotonation of C-16. Pathway (ii) initially forms the 14-membered cembrenyl cation with a 1,14-cyclization followed by a 1,3-hydride transfer (C-1 to C-15), 1,10-ring closure, and 1,5-hydride transfer (C-15 to C-11) prior to final deprotonation. We used an isotopic labeling experiment[17] to support the hydride shift from C-1 to C-11. We biosynthesized 1,1-$^2H_2$-GGPP in situ for incubation with Bnd4 (Figure S4). The deuterated enzymatic product was isolated, purified, and spectroscopically characterized using GC-MS and NMR. The M^+ peak and several fragments showed *m/z* values that were two Da higher than that of unlabeled **1** (Figures S5). The ^1H NMR of $^2H_2$-**1** was identical to that of **1** (ref. [7]) with the exception that the signals for H-1 (2.45 ppm) and H-11 (1.69 ppm) were absent and the doublet for CH_3-18 was a singlet (Figures S6–S8 and Table S4). The HSQC correlations between C-1 and H-1 and C-11 and H–11 also disappeared (Figures 2B, 2C, and S9). Together, it is clear that both deuterium atoms are retained and that one deuterium atom from C-1 in 1,1-$^2H_2$-GGPP migrates to C-11 in $^2H_2$-**1**. The labeling result, together with the *cis* configuration of C-15 and C-18, indicate pathway (i) is more probable than pathway (ii).

To further assess the two proposed pathways,[18] we performed quantum chemical calculations (mPW1PW91/6-31+G(d,p))[19–24] to calculate the relative free energies of cationic intermediates and transition state structures.[25] Predicted relative energies of the proposed intermediates in pathway (i) support a feasible downhill pathway with the allylic cation $\mathbf{B}^+$ 6.5 kcal mol^{-1} lower in energy than the 10-membered monocyclic intermediate $\mathbf{A}^+$ and the 6,10-bicyclic intermediate $\mathbf{C}^+$ another 5.1 kcal mol^{-1} lower (Figure 3). The bonds formed from the 1,10- and 1,14-cyclizations are elongated to 1.68 Å and 1.63 Å,

respectively, by hyperconjugation.[26] Pathway (ii) is predicted to be less favorable as the intermediate formed from 1,14-cyclization and 1,3-hydride shift is ~5 kcal mol^{-1} lower in energy than the 6,10-bicyclic intermediates that would follow (Figure S10), increasing the likelihood that premature deprotonation would occur if this pathway occurred. In addition, it appears that a *cis* C10–C11 alkene would be required as precursor to form the 6,10-bicycle with the naturally occurring relative configuration and in an energetically viable conformation.

Next, we investigated the catalytic importance of several residues in Bnd4. Canonical type I TSs are well known to possess two highly conserved metal-binding motifs, an Asp-rich DDxxD motif and an NSE or DTE triad.[27–29] Preliminary sequence analysis of Bnd4 revealed a D^{122}DxxD motif and an N^{234}DMFSFRAE triad, as well as the conserved W^{316}xxxxxR^{322}Y motif that is proposed for guiding diterpene synthase product formation (W) and, along with the conserved R188, sensing the diphosphate moiety (RY dyad).[7,29–31] Comparison of Bnd4 with homologues of Bnd4 (>50% sequence identities) revealed that the DDxxD motif is not strictly conserved (e.g., NDxxD, DDxxV, or GNxxA); the Bnd4 homologue from *Amycolatopsis arida* (DDxxV) retained benditerpe-2,6,15-triene synthase activity.[7] To test the requirement of this DDxxD motif, we made a D122A/D123A/D126A triple mutant (Figure S11) but TS activity was only minorly impaired (Figure 4). This finding led us to search for another putative metal-binding motif. We identified a putative Asp-rich motif, D^{94}NxxxD, upstream of the superfluous DDxxD motif. D94A, N95A, and D99A mutants revealed that D94A completely abolished activity while N95A and D99A were 41% and 71% active, respectively. This DNxxxD motif is strictly conserved amongst the Bnd4 homologues (Figure 4), and although some Asp-rich motifs in functional TSs deviate from the canonical DDxxD (e.g., DDxxE, DDxxxD, DDxD), DNxxxD has not been noted as a functional Asp-rich motif in TSs.[27–29]

We then implemented a random mutation screen to identify other key residues in Bnd4 (Figure S12). This system was employed given that the closest homologue of Bnd4 found in the PDB database, a thermostable ancestral version of spiroviolene synthase (PDB 6TBD),[15] was only 22.6% identical with 94% coverage (based on primary sequence). Of the randomly selected two hundred transformants, six transformants, R357G, E175G, S172F/I222V, D10V/S27G/D33A, V117M/L163P/Y248H, and E169K, showed evident influence on the production of **1** and were selected for further expansion of mutations (Figure 4). Mutation of E169 to Lys, Ala, Asp, Gln, Cys, or His completely abolished TS activity, showing its requirement for catalysis (Figure 4). Considering the negative charge of E169, we hypothesize that E169 likely helps to chelate Mg^{2+} in the active site, although the length of the side chain appears to be important since E169D was not active. E169 corresponds to E184 in the di-TS spatadiene synthase and E159 in the sesqui-TS selinadiene synthase, both of which were also proposed for Mg^{2+} binding.[12,32] Supported by the complete loss of activity of R173A, R173 may directly interact with the negatively charged diphosphate of the substrate (Figure 4). All other mutants tested (Figure S11) decreased the cyclase activity up to 5-fold but did not alter product specificity (Figure 4). In addition, we also used site-directed mutagenesis to change three conserved His residues (H229, D308, and H328) into Ala or Phe as His residues may act as a general base for final deprotonation in

TSs.[33–36] TS activity for both H328A and H328F was only minorly diminished suggesting aromaticity at position 328 is not required; no negative effect on catalysis was seen for H229 while H308A was insoluble (Figure 4). Additional experiments are required to identify the residue that facilitates deprotonation.

To assess the occurrence and conservativity of the unique DNxxxD motif, we performed a detailed bioinformatics analysis of Bnd4 and TSs within a range of 20–40% identities (i.e., not Bnd4 homologues). First, a neighbor-joining phylogenetic tree was constructed (Figure S13). Proteins within the Bnd4 clade were then used for motif discovery using the MEME suite.[37] The DNxxxD and the highly conserved NDxxSxxxE and WxxxxxRY motifs were all identified (Figure 4B). Within the Bnd4 clade, the consensus Asp-rich motif is (D/E)(N/D)xxx(D/Q) with the negative charge of the first D/E strictly conserved (Figure 4C). Notably, preliminary sequence analysis among other clades indicated additional variance in the DDxxD motif (Figure S13).

Finally, after attempts to obtain a crystal structure of Bnd4 failed, we built a model of Bnd4 for structural analysis and docking studies. Given that the most homologous proteins found in the PDB are below 23% identities, well below the 30% limit required to build a convincing homology model,[21,38] we created a model of Bnd4 using the tFold ‘de novo folding’ method.[39] The all α-helical structure resembled a typical type I TS structure (Figures 4 and S14) and Cα alignment with spiroviolene synthase gave a root-mean-square deviation of 1.402 Å. In addition, the DNxxxD motif, NSE triad, and other conserved residues are all reasonably found in a central active site (Figure 4D). We docked GGPP into the Bnd4 model and highlight one conformation that appears plausible for the formation of **1** with distances of C-1–C-10 and C-1–C-14 of 3.9 Å and 5.2 Å, respectively (Figure 4D). Residues near the diphosphate moiety of GGPP include D94 of the DNxxxD motif, E169, R173, the diphosphate sensor R188, N234 and E242 of the NSE motif, and the R322Y dyad. It should be noted that Mg^{2+} was not modeled and the presence of three Mg^{2+} ions may impact the placement of some of these side chains. A series of nonpolar residues, W67, L90, F162, V192, M194, Y197, and W316, form the hydrophobic chamber that supports 6,10-bicyclic ring formation (Figure 4D). Overall, this model and docking result is reasonable and supports the importance of the residues mentioned above, particularly D94 and E169.

In conclusion, Bnd4, the first characterized di-TS that produces the 6,10-bicyclic eunicellane skeleton, is a novel di-TS in both sequence and function. While its primary function is the formation of **1** in the biosynthesis of benditerpenoic acid,[7] it is also capable of cyclizing FPP and prenylating small nucleophiles using DMAPP or GPP. However, it is unknown if either of these reactions occur in vivo.[11] Our work supports a mechanistic proposal for the cyclization of the eunicellane skeleton where 1,10-cyclization precedes 1,14-cyclization. Similar mechanisms were proposed in the cyclizations of catenul-14-en-6-ol and hydropyrene, although **1** is not formed by the bacterial di-TSs catenul-14-en-6-ol synthase (CaCS) or hydropyrene synthase (HpS).[40,41] In fact, Bnd4 shares only 23% identities with both CaCS (52% coverage) and HpS (85% coverage). This cyclization timing is also in contrast to the proposed mechanisms for the marine 2,11-cyclized cembranoids[2] and the bacterial diterpene spiroalbatene,[42] which are all proposed to form

the 14-membered cembrane skeleton prior to 1,10-cyclization; the former is also proposed to undergo isomerization of GGPP to geranyllinalyl diphosphate to yield a *Z*-configured alkene. Finally, the stereochemical configuration of the four stereocenters at 1, 10, 11, and 14 in the eunicellane skeleton is also a major consideration of how these enzymes fold their cationic intermediates. Comparative studies with other eunicellane-forming TSs, once they are identified, will be of high interest. Bacteria are an excellent source of structurally unique and biologically active terpenoids[43] and genome mining for new TSs in bacteria, particularly TSs with unique Asp-rich motifs and non-canonical TSs,[44] will surely lead to the discovery of new TSs that generate novel terpene skeletons and new natural products.

Supplementary Material

Refer to Web version on PubMed Central for supplementary material.

Acknowledgements

This work was funded in part by NIH Grant R00 GM124461 and the University of Florida (to J.D.R.) and NSF Grants CHE-1856416 and CHE-030089 (XSEDE) (to D.J.T.). We thank Prof. Sandra Loesgen for helpful discussions and for providing *Streptomyces* sp. (CL12-4). We thank Prof. C. Dale Poulter for the gifts of 1,1-$^{2}H_{2}$-DMAPP and FPP. We also thank Prof. Sixue Chen for providing *Arabidopsis* cDNA. We acknowledge the University of Florida Mass Spectrometry Research and Education Center (MSREC), which is supported by the NIH (S10 OD021758-01A1), and Jodie Johnson for GC-MS support, and the University of Florida Center for Nuclear Magnetic Resonance Spectroscopy for NMR support. We thank Prof. Chin-Yuan Chang for crystallization attempts of Bnd4.

References

[1]. Dictionary of Natural Products, http://dnp.chemnetbase.com, accessed May 16, 2021.

[2]. Li G, Dickschat JS, Guo YW, Nat. Prod. Rep 2020, 37, 1367–1383. [PubMed: 32458945]

[3]. Welford AJ, Collins I, J. Nat. Prod 2011, 74, 2318–2328. [PubMed: 21970540]

[4]. Bernardelli P, Paquette LA, Heterocycles 1998, 49, 531–556.

[5]. Pinto AC, Pizzolatti MG, De Epifanio RA, Frankmölle W, Fenical W, Tetrahedron 1997, 53, 2005–2012.

[6]. Zhang BY, Wang H, Luo XD, Du ZZ, Shen JW, Wu HF, Zhang XF, Helv. Chim. Acta 2012, 95, 1672–1679.

[7]. Zhu C, Xu B, Adpressa DA, Rudolf JD, Loesgen S, Angew. Chem., Int. Ed 2021, 60, 14163–14170.

[8]. Ma LF, Chen MJ, Liang DE, Shi LM, Ying YM, Shan WG, Li GQ, Zhan ZJ, J. Nat. Prod 2020, 83, 1641–1645. [PubMed: 32367724]

[9]. Al Batal M, Jones PG, Lindel T, Eur. J. Org. Chem 2013, 2013, 2533–2536.

[10]. Frichert A, Jones PG, Lindel T, Beilstein J Org. Chem 2018, 14, 2461–2467.

[11]. Xu B, Li Z, Alsup TA, Ehrenberger MA, Rudolf JD, ACS Catal. 2021, 11, 5906–5915.

[12]. Rinkel J, Lauterbach L, Dickschat JS, Angew. Chem., Int. Ed 2017, 56, 16385–16389.

[13]. Dickschat JS, Pahirulzaman KAK, Rabe P, Klapschinski TA, ChemBioChem 2014, 15, 810–814. [PubMed: 24573945]

[14]. Rinkel J, Lauterbach L, Dickschat JS, Angew. Chem., Int. Ed 2019, 58, 452–455.

[15]. Schriever K, Saenz-Mendez P, Rudraraju RS, Hendrikse NM, Hudson EP, Biundo A, Schnell R, Syrén PO, J. Am. Chem. Soc 2021, 143, 3794–3807. [PubMed: 33496585]

[16]. Kim SY, Zhao P, Igarashi M, Sawa R, Tomita T, Nishiyama M, Kuzuyama T, Chem. Biol 2009, 16, 736–743. [PubMed: 19635410]

[17]. Dickschat JS, European J. Org. Chem 2017, 2017, 4872–4882.

[18]. Hong YJ, Tantillo DJ, Chem. Sci 2010, 1, 609–614.

[19]. Adamo C, Barone V, J. Chem. Phys 1998, 108, 664–675.

[20]. All structures were fully optimized (and confirmed as minima or transition state structures through vibrational analysis) and free energies were computed at this level of theory, which has been validated previously as appropriate for terpene-forming carbocation rearrangemnents (even when occurring in enzyme active sites); see, for example Refs. 21–24.

[21]. Tantillo DJ, in Comprehensive Natural Products III: Chemistry and Biology (Eds.: Liu HW, Begley TP), Elsevier, 2020, pp. 644–563.

[22]. Matsuda SPT, Wilson WK, Xiong Q, Org. Biomol. Chem 2006, 4, 530–543. [PubMed: 16446812]

[23]. Tantillo DJ, Nat. Prod. Rep 2011, 28, 1035–1053. [PubMed: 21541432]

[24]. Tantillo DJ, Angew. Chem., Int. Ed 2017, 56, 10040–10045.

[25]. A data set collection of computational results is available in the IoChem-BD repository and can be accessed via DOI:10.19061/Iochem-Bd-6-92.

[26]. Tantillo DJ, Chem. Soc. Rev 2010, 39, 2847–2854. [PubMed: 20442917]

[27]. Christianson DW, Chem. Rev 2017, 117, 11570–11648. [PubMed: 28841019]

[28]. Dickschat JS, Nat. Prod. Rep 2016, 33, 87–110. [PubMed: 26563452]

[29]. Dickschat JS, Angew. Chem., Int. Ed 2019, 58, 2–15.

[30]. Driller R, Janke S, Fuchs M, Warner E, Mhashal AR, Major DT, Christmann M, Brück T, Loll B, Nat. Commun 2018, 9, 3971. [PubMed: 30266969]

[31]. Rabe P, Schmitz T, Dickschat JS, Beilstein J. Org. Chem 2016, 12, 1839–1850. [PubMed: 27829890]

[32]. Baer P, Rabe P, Fischer K, Citron CA, Klapschinski TA, Groll M, Dickschat JS, Angew. Chem., Int. Ed 2014, 53, 7652–7656.

[33]. Potter KC, Zi J, Hong YJ, Schulte S, Malchow B, Tantillo DJ, Peters RJ, Angew. Chemie - Int. Ed 2016, 55, 634–638.

[34]. Potter KC, Jia M, Hong YJ, Tantillo D, Peters RJ, Org. Lett 2016, 18, 1060–1063. [PubMed: 26878189]

[35]. Rudolf JD, Bin Dong L, Cao H, Hatzos-Skintges C, Osipiuk J, Endres M, Chang CY, Ma M, Babnigg G, Joachimiak A, Phillips GN, Shen B, J. Am. Chem. Soc 2016, 138, 10905–10915. [PubMed: 27490479]

[36]. Schrepfer P, Buettner A, Goerner C, Hertel M, Van Rijn J, Wallrapp F, Eisenreich W, Sieber V, Kourist R, Brück T, Proc. Natl. Acad. Sci. U. S. A 2016, 113, E958–E967. [PubMed: 26842837]

[37]. Bailey TL, Boden M, Buske FA, Frith M, Grant CE, Clementi L, Ren J, Li WW, Noble WS, Nucleic Acids Res. 2009, 37, W202–W208. [PubMed: 19458158]

[38]. Xiang Z, Curr. Protein Pept. Sci 2006, 7, 217–227. [PubMed: 16787261]

[39]. Xiao Q, Wang L, Supekar S, Shen T, Liu H, Ye F, Huang J, Fan H, Wei Z, Zhang C, Nat. Commun 2020, 11, 5430. [PubMed: 33110062]

[40]. Li G, Guo YW, Dickschat JS, Angew. Chem., Int. Ed 2021, 60, 1488–1492.

[41]. Rinkel J, Rabe P, Chen X, Köllner TG, Chen F, Dickschat JS, Chem. - A Eur. J 2017, 23, 10501–10505.

[42]. Rinkel J, Lauterbach L, Rabe P, Dickschat JS, Angew. Chem., Int. Ed 2018, 57, 3238–3241.

[43]. Rudolf JD, Alsup TA, Xu B, Li Z, Nat. Prod. Rep 2021, 38, 905–980. [PubMed: 33169126]

[44]. Rudolf JD, Chang CY, Nat. Prod. Rep 2020, 37, 425–463. [PubMed: 31650156]

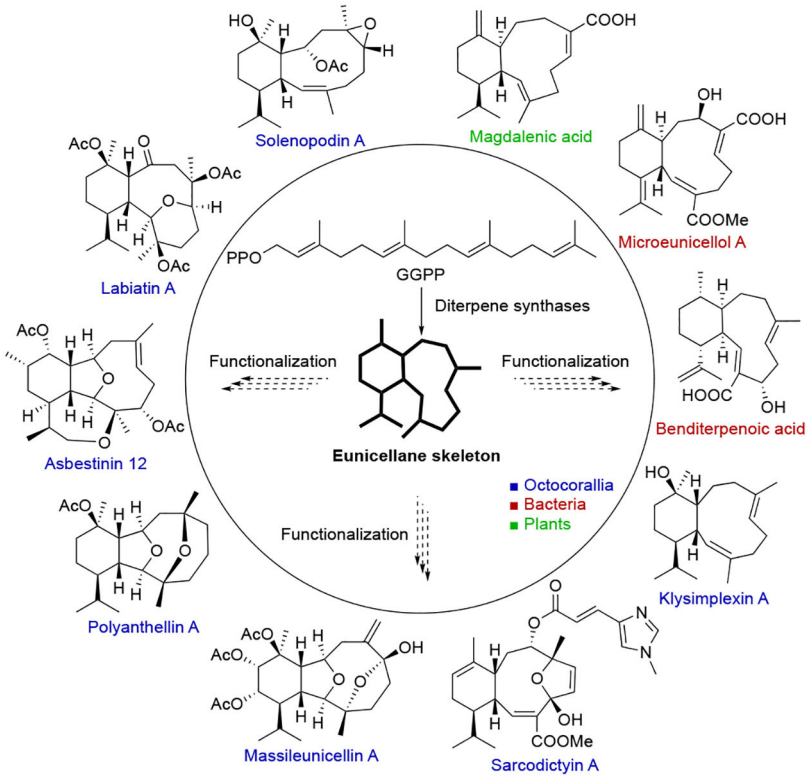

Figure 1.

Selected members of eunicellane diterpenoids. Di-TSs form the eunicellane skeleton and accessory enzymes functionalize the core to produce diverse natural products.

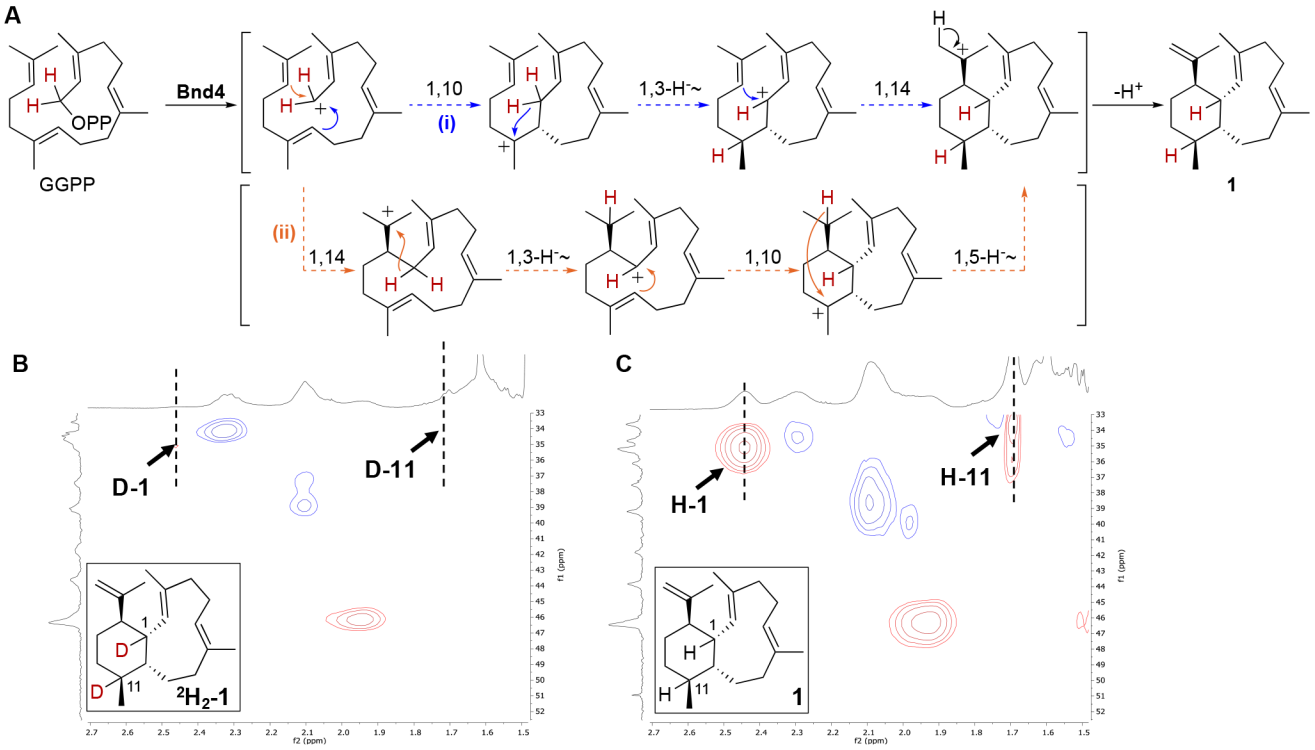

Figure 2.

Mechanistic proposals and deuterium labeling support for the cyclization of GGPP into **1**. (A) Two plausible pathways (i, blue) and (ii, orange) for the formation of the 6,10-bicyclic eunicellane skeleton. Red hydrogens atoms depict the deuterium atoms in the labeling experiment. (B and C) ^{1}H-^{13}C HSQC spectra of $^2H_2$-**1** and **1**, respectively. Full NMR spectra in Figures S6– S9.

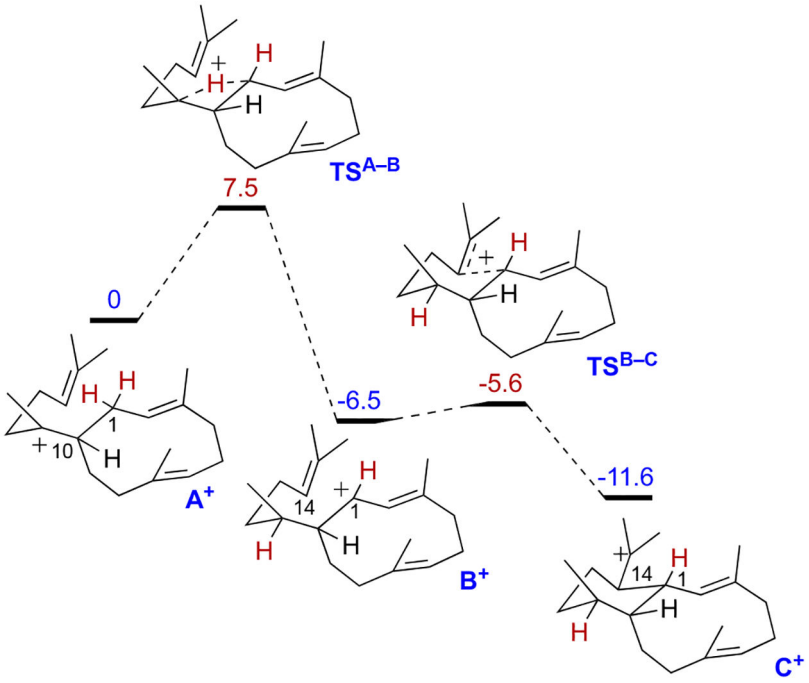

Figure 3.

Relative free energies of intermediates and transition state structures in kcal mol^{-1}, calculated with mPW1PW91/6-31+G(d,p).[19–24] Blue and red values are relative energies for minima and transition state structures, respectively. The conformations depicted here for the pendant chain in **A**$^+$, $TS^{A\text{-}B}$, and B+ are qualitative; see computed structures for actual conformations.[25]

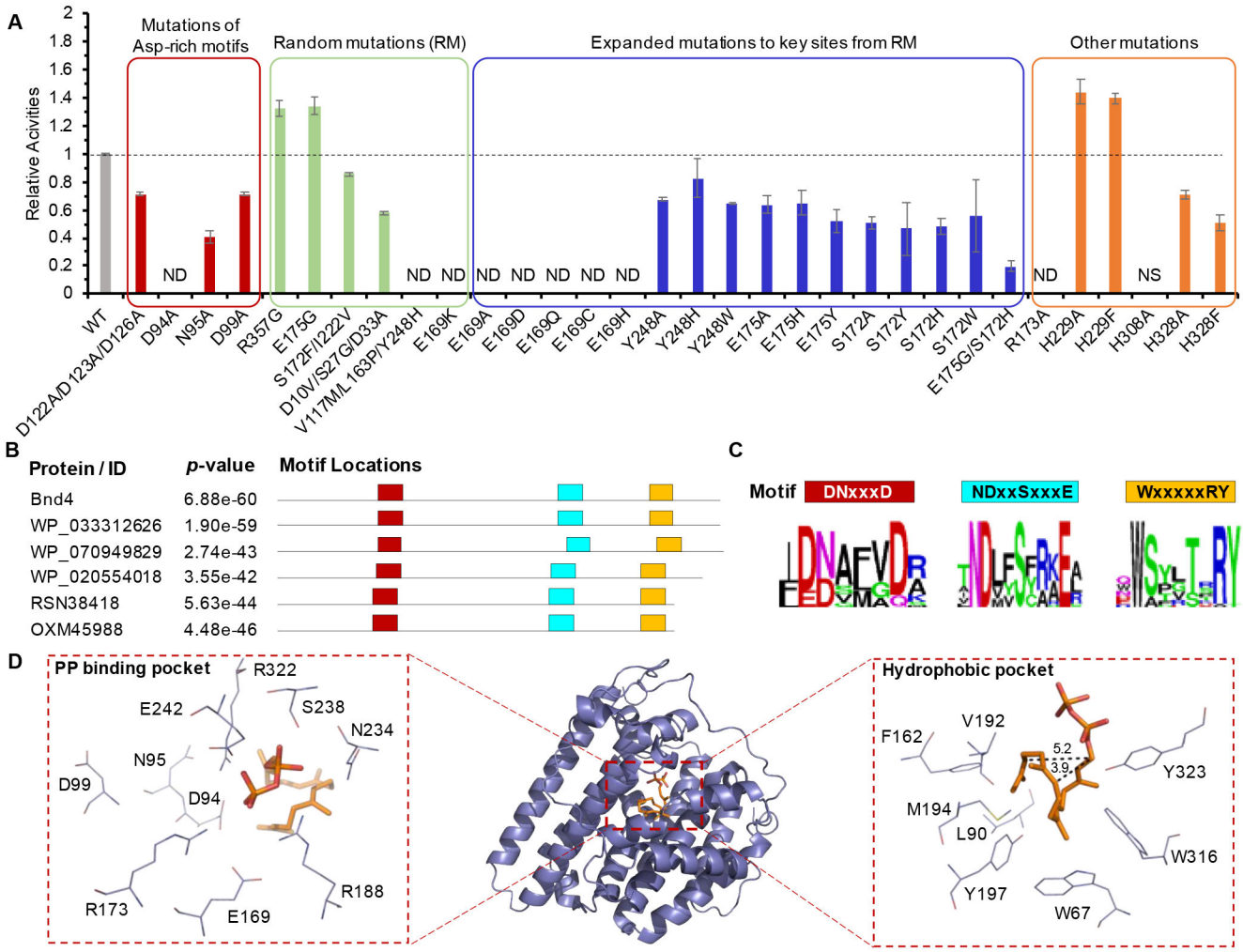

Figure 4.

Mutational, bioinformatics, and structural analysis of Bnd4. (A) Relative cyclization activities of Bnd4 and mutants. The activity of WT Bnd4, corresponding to a relative activity of 1, is 14.6 ± 0.1 nmol mg^{-1} min^{-1}. ND and NS denote not detected and not soluble, respectively. (B and C) Sequence analysis of Bnd4 and selected homologues highlighting the DNxxxD, NSE, and WxxxxxRY motifs. See Supporting Information for *p*-value definition. (D) Structural model of Bnd4 with displaying key active site residues (lines) and a docking model of GGPP (sticks); dashed lines are distances in Å.

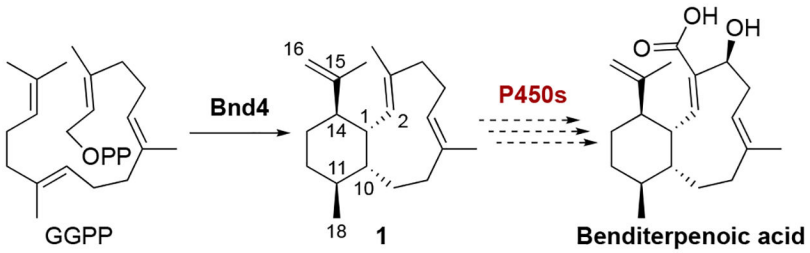

Scheme 1.